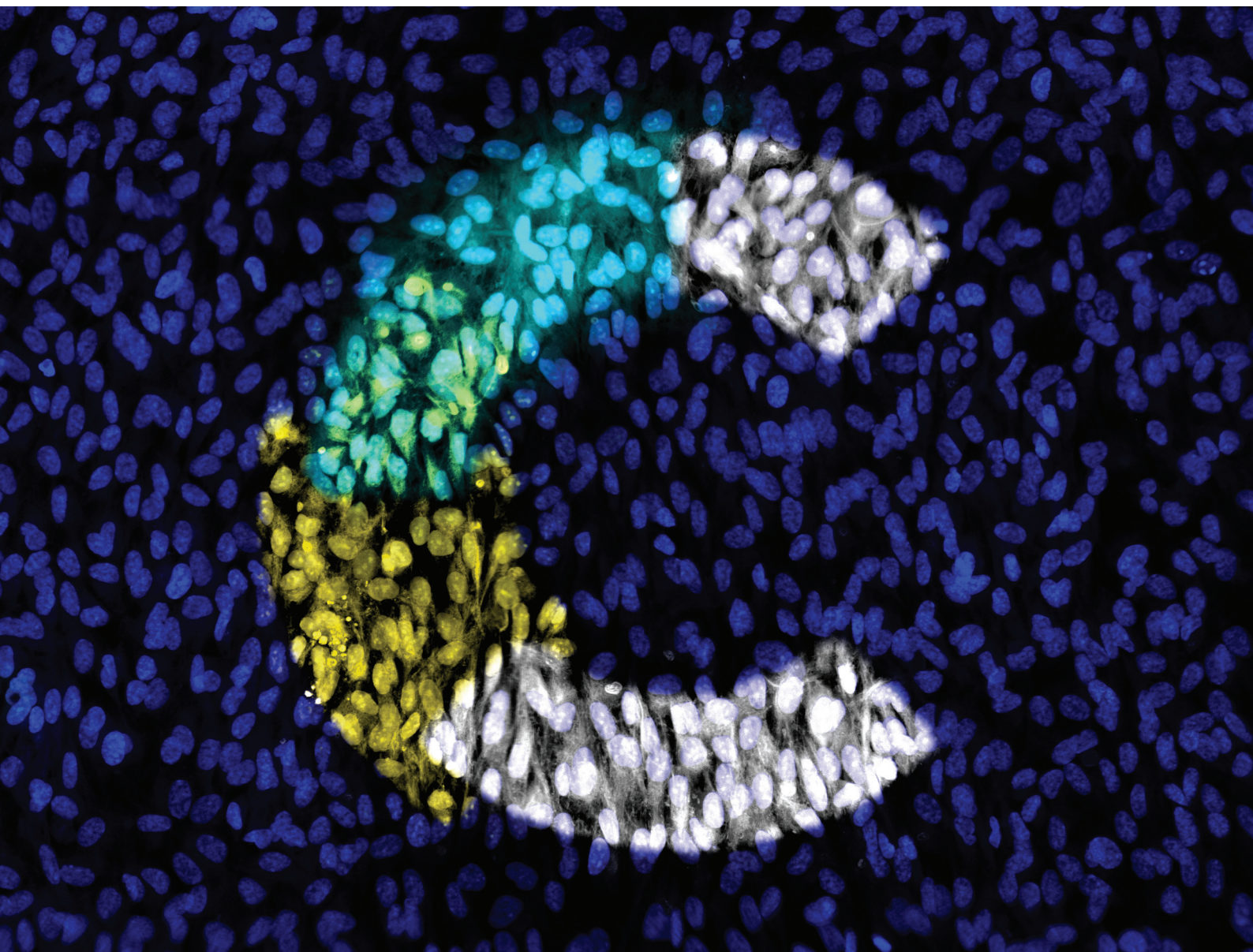


Organic & Biomolecular Chemistry

Volume 24
Number 1
7 January 2026
Pages 1-242

rsc.li/obc



ISSN 1477-0520

PAPER

Daniel Fürth *et al.*
Heterocyclic scaffold-fused dimethoxy-dibenzocyclooctynes
for photoactivatable click chemistry

Cite this: *Org. Biomol. Chem.*, 2026, **24**, 120

Heterocyclic scaffold-fused dimethoxy-dibenzocyclooctynes for photoactivatable click chemistry

N. Alfred Larsson, ^a Taegeun Jo, ^c Ulf Bremberg,^b Stefano Crespi, ^c Luke R. Odell ^b and Daniel Fürth *^{a,d}

Dibenzocyclooctynes (DBCOS) are widely used in bioorthogonal chemistry for strain-promoted azide–alkyne cycloaddition (SPAAC), but generally lack reactivity toward inverse–electron–demand Diels–Alder cycloaddition (iEDDAC) with tetrazines. While photoactivatable DBCOs for SPAAC are well established and photoresponsive cyclooctynes for iEDDAC have recently been reported, photoactivatable DBCOs designed for dual reactivity remain scarce. Motivated by the possibility that heterocyclic fusions could tune reactivity and introduce new photochemical properties, we developed a modular synthetic route to a previously inaccessible heterocycle–fused DBCO. Upon photoactivation, the pyrrolidine fusions efficiently released the alkyne from the cyclopropenone cage, exhibiting strong SPAAC reactivity but, contrary to computational predictions, showing no detectable reactivity with tetrazines in iEDDAC. By contrast, triazole fusions, previously described as fluorogenic dibenzocyclooctyne (FL–DIBO), have not been evaluated in photo–click chemistry. We found that the cyclopropenone cage is essential for fluorescence, and its decarbonylation produced non–alkyne byproducts with no functional reactivity. This work expands the chemical space of DBCOs and establishes pyrrolidine–fused derivatives as the first functional heterocyclic–fused photoactivatable alkyne within the dimethoxy–DBCO scaffold class.

Received 11th August 2025,
Accepted 20th October 2025

DOI: 10.1039/d5ob01314c

rsc.li/obc

Introduction

The strain-promoted azide–alkyne cycloaddition (SPAAC)^{1,2} and the inverse electron-demand Diels–Alder cycloaddition (iEDDAC)³ are two of the most widely used copper-free click reactions in chemical biology. Dibenzocyclooctyne (DBCO) is a prominent SPAAC reagent, valued for its high reactivity with azides and broad utility in bioconjugation. In parallel, iEDDAC reactions commonly employ strained alkenes such as *trans*-cyclooctene (TCO), which displays exceptionally fast kinetics with tetrazines and has become a mainstay in bioorthogonal labeling. These two reactions are generally considered mutually orthogonal, forming the basis for many dual-labeling strategies.

Expanding the structural diversity of strained alkynes has been a productive route to tuning reactivity and orthogonality. Bicyclononyne (BCN), which features a cyclopropane-fused cyclooctyne core, is notable for its ability to undergo both SPAAC with azides and iEDDAC with tetrazines.^{4,5} Inspired by

BCN's dual reactivity, Mayer *et al.* introduced a cyclopropene fusion onto the dibenzocyclooctyne scaffold, which surprisingly endowed the resulting compound with tetrazine reactivity.⁶ This finding challenged the assumption that DBCO derivatives are inert toward tetrazines and highlighted how subtle ring modifications can dramatically reshape reactivity in bioorthogonal chemistry.

Building on these insights, Svatunek and colleagues recently used density functional theory (DFT) calculations to predict that certain cycloalkane-fused DBCO derivatives, such as cyclopentane-DMBO (5C-DMBO), could exhibit enhanced reactivity toward tetrazines while retaining SPAAC reactivity⁷ (Fig. 1a). Motivated by these computational predictions, we have developed a novel synthesis of a pyrrolidine-fused DMBO derivative closely resembling the predicted 5C-DMBO structure (Fig. 1c). A key limitation of the cyclopentane-fused DMBO (5C-DMBO) scaffold is the absence of a heteroatom handle for straightforward functionalization onto biomolecules. In contrast, the cyclopropane-fused DMBO (3C-DMBO) synthesized by Mayer *et al.* includes such a handle, but at the cost of a significantly more complex and lengthy synthetic route (see SI Fig. S2 for comparison). Our approach introduces a pyrrolidine ring fused to the DMBO core, providing a heterocyclic nitrogen atom that can, in principle, serve as a convenient handle for further derivatization. This modular strategy not only

^aDepartment of Immunology, Genetics & Pathology, Uppsala University, SE-751 85 Uppsala, Sweden. E-mail: furth@scilifelab.uu.se^bDepartment of Medicinal Chemistry, Uppsala University, Uppsala, Sweden^cDepartment of Chemistry, Uppsala University, Uppsala, Sweden^dScience for Life Laboratory (SciLifeLab), Uppsala University, Uppsala, Sweden

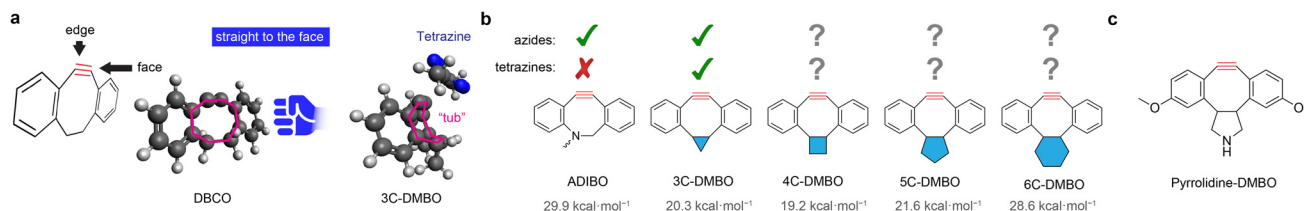


Fig. 1 Rational engineering of scaffold-fused DBCOs for iEDDAC reactivity. (a) Chemical structure of dibenzocyclooctynes illustrating the “edge” and “face” approach trajectories of an incoming reactant. A three-dimensional model of DBCO demonstrates that inverse electron-demand Diels–Alder (iEDDAC) reactivity requires a direct “face-on” approach, analogous to a punch to the face. However, this trajectory is sterically hindered in the native scaffold, preventing productive ligation. Incorporation of a cycloalkane fusion, as in 3C-DMBO,⁷ induces a more open, “tub-like” conformation that accommodates face-on approach and lowers the activation barrier, thereby enabling efficient tetrazine ligation. (b) Previously suggested hypothetical dibenzocyclooctyne derivatives.⁶ DFT-calculated activation energies for the reaction with tetrazine, taken from Svatoněk and colleagues,⁷ are shown below each compound. ADIBO reacts exclusively with azides, while Mayer *et al.*⁶ showed 3C-DMBO reacts with both azides and tetrazines. Although untested experimentally, computational results predict that 4C-DMBO and 5-DMBO will also react with these partners. (c) Chemical structure of pyrrolidine-DMBO introduced in this work.

simplifies access to these heterocycle-fused DBCO derivatives but also opens new avenues for functionalization and conjugation in bioorthogonal applications. This route achieves a sixteen-fold higher yield compared to the original photo-DMBO synthesis, significantly improving access to this chemical space. Contrary to computational predictions, the synthesized compound retains efficient reactivity toward azides but shows no measurable reaction with tetrazines under conditions where DMBO undergoes rapid iEDDAC. This highlights how subtle differences in heterocyclic structures, compared to cycloalkanes, can significantly influence reactivity profiles. Understanding these nuances is crucial for the rational design of bioorthogonal reagents with predictable performance.

Results

Feasibility of synthesizing DMBO derivatives

The recently reported photo-DMBO scaffold exhibits an exceptionally low overall yield of just 0.5%, highlighting a significant synthetic bottleneck despite its promising bioorthogonal reactivity.⁶ This challenge underscores the need for improved synthetic strategies to access similarly reactive dibenzocyclooctyne derivatives with more practical yields. Computational predictions have suggested that fusing carbocyclic rings to the DMBO core can enhance tetrazine reactivity by stabilizing more favorable geometries, identifying a series of four-, five-, and six-membered ring fused DMBO derivatives as promising candidates⁷ (Fig. 1b). Among these, the four-membered ring fused derivative (4C-DMBO) showed the lowest predicted activation barrier for the inverse-electron-demand Diels–Alder reaction (19.2 kcal mol⁻¹ compared to 20.3 kcal mol⁻¹ for DMBO).⁷ Such highly strained carbocycles are notoriously difficult to synthesize due to limited synthetic routes compared to flexible, strain-free propane linkers – making the most reactive predicted structure also the least accessible. The six-membered ring derivative (6C-DMBO) exhibited predicted activation energies comparable to ADIBO, a scaffold known to be unreactive towards tetrazines, leaving the five-membered

ring derivative (5C-DMBO) as the most promising candidate for improved synthesis.

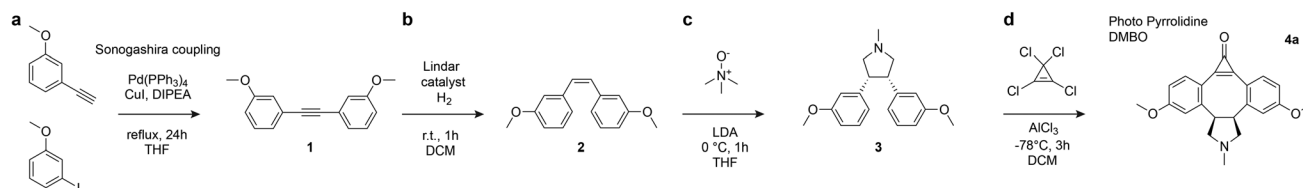
To this end, we pursued the synthesis of a pyrrolidine-functionalized DMBO (pyrrolidine-DMBO), replacing the carbocyclic 5C-DMBO ring with a five-membered nitrogen heterocycle to both retain the strained geometry required for reactivity while also introducing a handle for convenient functionalization onto biomolecules of interest (Fig. 1c). This approach facilitates ring formation *via* a [3 + 2] cycloaddition between an alkene and trimethylamine *N*-oxide,⁸ providing a straightforward and modular approach to the fused system. Lastly, the incorporation of nitrogen offers additional sites for functional modification, while preserving the key structural features suggested by the original computational model.

Our suggested synthesis path can be broken down into four steps (Scheme 1). First, 1-ethynyl-3-methoxybenzene and 3-iodoanisole undergo an alkyne-aryl halide cross-coupling reaction (Scheme 1a). The internal alkyne is then selectively reduced to a *cis*-alkene using H₂ and Lindlar catalyst in DCM (Scheme 1b). Next, the resulting stilbene derivative was reacted with an azomethine ylide formed from trimethylamine *N*-oxide using lithium diisopropylamide (LDA) in THF at 0 °C, forming the pyrrolidine-fused product⁸ (Scheme 1c). Finally, the key photoreactive cyclopropenone motif^{9,10} (Scheme 1d) was installed *via* an intramolecular Friedel–Crafts alkylation with tetrachlorocyclopropene.

Pyrrolidine-DMBO retains azide reactivity but shows no reactivity towards tetrazines

To assess the orthogonal reactivity of the synthesized pyrrolidine-DMBO, we conducted LCMS experiments with 2-azidoethanol and 3,6-dimethyltetrazine (Fig. 2a). Pyrrolidine-DMBO reacted efficiently with 2-azidoethanol, yielding the expected triazole product and confirming efficient SPAAC performance (Fig. 2b). However, no iEDDAC reaction was observed when 3,6-dimethyltetrazine was treated with pyrrolidine-DMBO under identical conditions (Fig. 2c). This is in contrast with recent computational predictions of high tetrazine reactivity for fused five-membered DBMO derivatives.⁷





Scheme 1 Synthesis of photo-caged pyrrolidine-DMBO. (a) Compound **1** was prepared via a Sonogashira cross-coupling reaction between 3-iodoanisole and 3-ethynylanisole. (b) Compound **2** was prepared by hydrogenation in presence of Lindlar catalyst. (c) Compound **3** was prepared via [3 + 2] cycloaddition with trimethylamine *N*-oxide. (d) Photo-pyrrolidine-DMBO (**4a**) was prepared via an intramolecular Friedel-Crafts alkylation with tetrachlorocyclopropene.

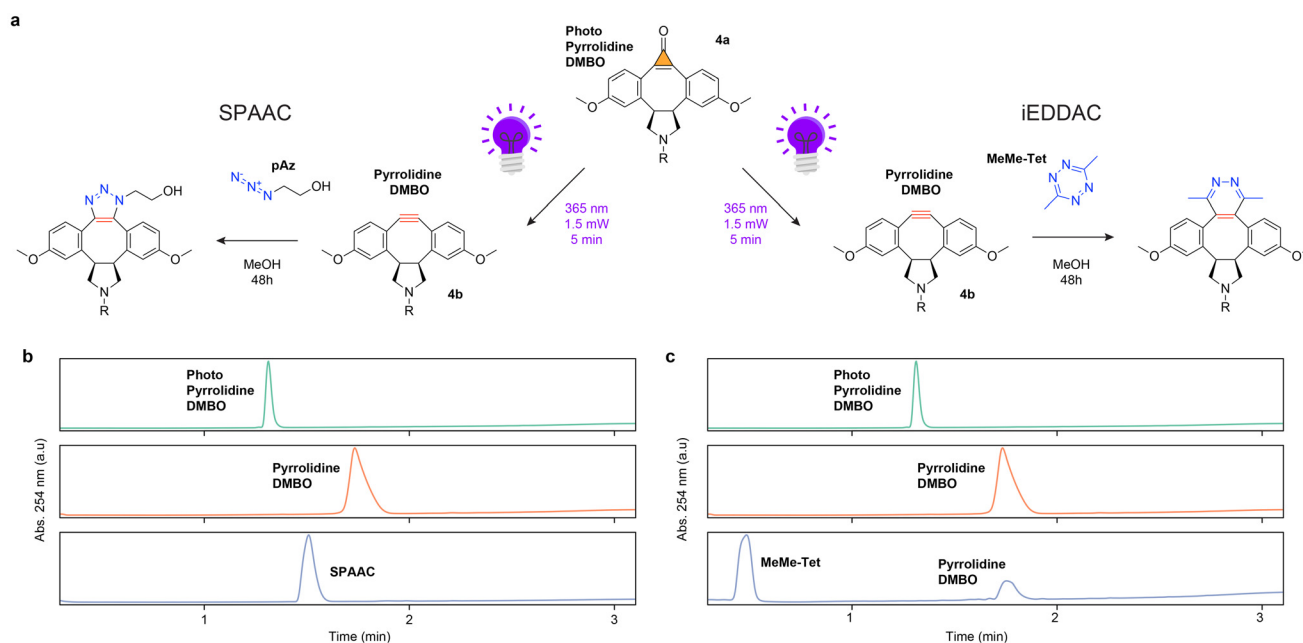


Fig. 2 Pyrrolidine-DMBO reacts with azides but not with tetrazines. (a) Experimental design. Each experimental branch starts out with a pyrrolidine-DMBO with an intact cyclopropanone photocage (photo-pyrrolidine-DMBO). The cyclopropanone cage is decarbonylated by exposure to 1.5 mW of UV light (365 nm wavelength) for 5 minutes resulting in pyrrolidine-DMBO. Lastly either 2-azidoethanol (pAz) or 3,6-dimethyltetrazine (MeMe-Tet) is added and both reactions are allowed to run for 48 hours at room temperature in methanol (MeOH). (b) Liquid-chromatography mass spectrometry (LC-MS) analysis reveals that only pyrrolidine-DMBO shows SPAAC reactivity towards pAz. (c) But no iEDDAC reactivity towards MeMe-Tet; reaction conditions: 250 μ M cyclooctyne, 2.5 mM pAz or MeMe-Tet, room temperature in methanol, 48 hours.

This discrepancy may be attributable to problems encountered during synthesis. More specifically, one plausible explanation that reconciles the computational predictions with the observed lack of tetrazine reactivity (despite retained azide reactivity) is that epimerization occurred during or before pyrrolidine ring formation, resulting in the formation of a *trans*-fused rather than the intended *cis*-fused system. To evaluate this possibility, we analyzed the compound by proton nuclear magnetic resonance (^1H NMR) spectroscopy. To assign the configuration of photo-pyrrolidine-DMBO, we performed conformational analysis and NMR simulations with Boltzmann averaging over all conformers (see SI for details). The predicted ^1H - ^1H coupling constants between 2H and 6H are 0.4 Hz (*trans*) and 7.0 Hz (*cis*), compared to the experimental values of 4.3 Hz and 6.7 Hz (Fig. S5). Predicted chemical shifts also distinguish the isomers: the *cis*-isomer shows three symmetric

signals, while the *trans*-isomer shows six asymmetric signals. The experimental spectrum displays symmetric shifts, confirming the *cis*-fused configuration (Fig. 3). These results indicate that the lack of tetrazine reactivity cannot be attributed to ring fusion geometry, as the *cis* isomer is present rather than the *trans*.

Lastly, we considered whether the lack of tetrazine reactivity could be attributed to solvent effects or other reaction conditions. Since the original experiments were carried out under conditions analogous to those reported previously⁷ (specifically in methanol) we repeated the reaction under different solvent conditions to evaluate the potential influence of solvent polarity, ionic strength, or protonation state of the amine. We performed the reaction in an aprotic solvent (DMSO) supplemented with a non-nucleophilic base (DIPEA, 1 eq.) to ensure that the secondary amine remains neutral and



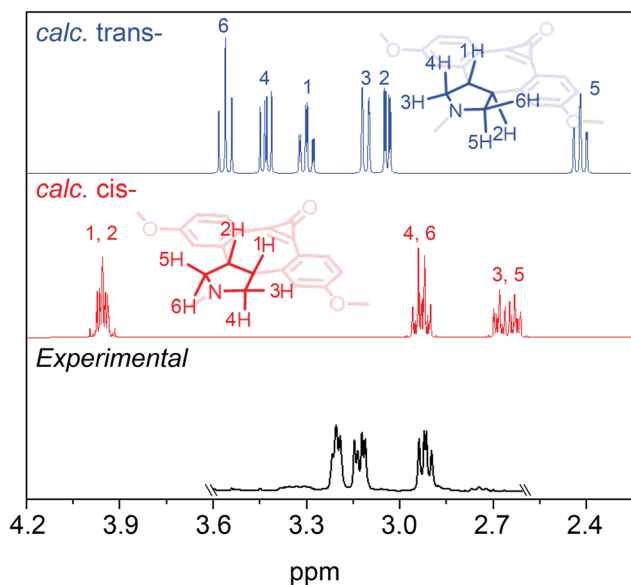


Fig. 3 Comparison of simulated and experimental ^1H NMR spectra for photo-pyrrolidine-DMBO. Simulated spectra for the *trans*- and *cis*-fused isomers are shown in blue and red, respectively, with the experimental spectrum overlaid in black. The *cis*-isomer exhibits three sets of symmetric signals, whereas the *trans*-isomer shows six distinct signals due to its asymmetric geometry. The experimental spectrum closely matches the *cis*-isomer, confirming the *cis*-fused configuration.

to minimize potentially unfavorable ionic interactions. Even under these conditions, no tetrazine reactivity was observed but SPAAC reactivity was retained (SI Fig. S3), reinforcing the conclusion that the absence of iEDDAC reactivity reflects an intrinsic limitation of the compound itself, rather than an artifact of solvent or reaction conditions.

Reduced SPAAC reaction rates for pyrrolidine-DMBO compared to azadibenzocyclooctyne

Azadibenzocyclooctyne (ADIBO) is the most widely used and commercially produced derivative of dibenzocyclooctyne (DBCO). The second-order rate constant for the ADIBO-azide cycloaddition in methanol has been consistently reported at approximately 0.3 to $0.4 \text{ M}^{-1} \text{ s}^{-1}$ by multiple independent groups.^{7,11} This reproducibility makes ADIBO a useful benchmark or “gold standard” for comparing the reactivity of newly developed cyclooctynes. The second-order kinetics of the reactions between pyrrolidine-DMBO or azadibenzocyclooctyne (ADIBO) and 2-azidoethanol were measured by monitoring the decrease in absorbance at 307 nm in methanol at room temperature. Time-resolved UV-Vis spectra were fitted to obtain second-order rate constants (Fig. 4 and Table 1).

Pyrrolidine-DMBO exhibited a significantly slower reaction rate ($k_2 = 0.04 \text{ M}^{-1} \text{ s}^{-1}$) compared to ADIBO ($k_2 = 0.34 \text{ M}^{-1} \text{ s}^{-1}$) under identical conditions, consistent with attenuated SPAAC kinetics ($b = -0.29 \text{ M}^{-1} \text{ s}^{-1}$, SE = $0.02 \text{ M}^{-1} \text{ s}^{-1}$, $t(7) = -13.10$, $p < 0.001$).

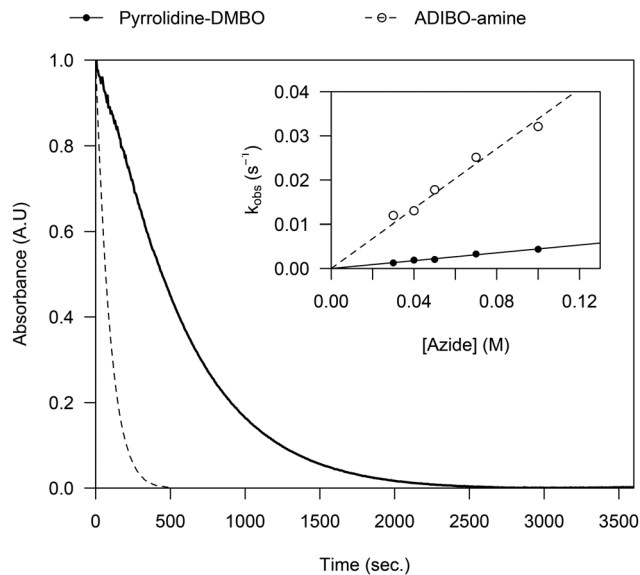


Fig. 4 Pyrrolidine-DMBO exhibits reduced SPAAC rates compared to ADIBO. Absorbance at 307 nm as a function of time for $100 \mu\text{M}$ pyrrolidine-DMBO (solid line) or ADIBOamine (dashed line) in the presence of 30 mM 2-azidoethanol. The inset shows the observed rate constants (k_{obs}) plotted against azide concentration ([azide]), with linear fits used to determine second-order rate constants. Pyrrolidine-DMBO (\bullet , solid line) exhibits significantly slower reaction kinetics compared to ADIBOamine (\circ , dashed line). Reactions were performed at 2-azidoethanol concentrations of 30, 40, 50, 70, and 100 mM .

Table 1 Second-order rate constants (k_2) for Pyrrolidine-DMBO and ADIBO-amine reactions with 2-azidoethanol in methanol

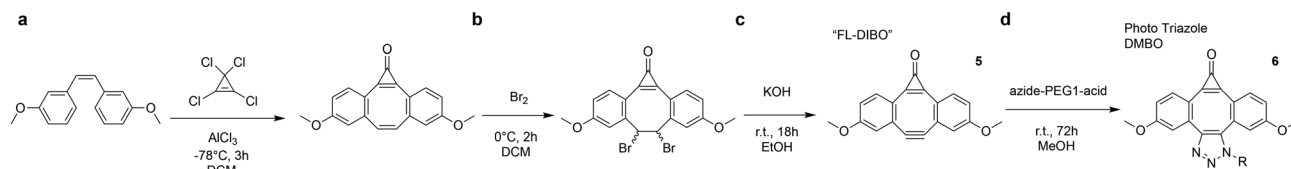
Compound	$k_2 \text{ (M}^{-1} \text{ s}^{-1}\text{)}$	Standard error	R_2
Pyrrolidine-DMBO	0.0444	± 0.0011	0.998
ADIBO-amine	0.3387	± 0.0108	0.996

These results indicate that incorporation of the pyrrolidine moiety decreases the cyclooctyne's reactivity towards azides relative to the standard ADIBO scaffold.

Fluorogenic triazole fusions undergo photodecarbonylation to radicals, preventing alkyne release

Boons and colleagues¹² were the first to synthesize a heterocyclic compound *via* a strategy analogous to the one we used for pyrrolidine, resulting in a triazole-fused dimethoxy-DIBO scaffold. To our knowledge, it has not yet been systematically tested whether decarbonylation of the cyclopropenone in FL-DIBO can generate a functional alkyne, and whether such an alkyne retains reactivity toward azides and tetrazines. We applied a similar synthetic scheme as Boons and colleagues,¹² introducing a PEG₁-acid linker through triazole fusion (Scheme 2). As previously reported, the resulting conjugate exhibits a strong absorption peak at 360 nm and a pronounced emission peak at 488 nm, effectively acting as a fluorophore (Fig. 5a). This stands in stark contrast to the pyrrolidine fusion, which is non-fluorescent. Next, we investigated





Scheme 2 Synthesis of fluorescent triazole-DMBO, the initial step is identical to step (a) in Scheme 1. Steps a–c are adapted from Friscourt *et al.*¹² resulting in what they refer to as fluorescent DIBO (FL-DIBO). R = PEG1-acid.

whether the cyclopropenone photocage could be removed to generate a reactive alkyne and whether this alkyne would undergo cycloaddition with azides and tetrazines. Following the irradiation protocol previously used for the pyrrolidine fusion, we first exposed the molecule to 5 minutes of 365 nm LED light at 1.5 mW, but the molecule remained fluorescent, and the cyclopropenone cage was intact. Given that prior studies identified the cyclopropenone group as critical for fluorescence,¹² this suggested that longer irradiation, sufficient to bleach the fluorophore, might be required. We therefore increased the irradiance to 3 mW and irradiated for 100 minutes, monitoring the reaction every 5 minutes by fluorescence and LC-MS, which revealed decarbonylation of the cyclopropenone cage. Unfortunately, immediately upon decarbonylation, we observed radical generation and detected no formation of the expected cyclooctyne, as indicated by both LC-MS and a subsequent SPAAC reaction. Unsurprisingly, no iEDDAC reaction was observed either (Fig. 5b). To minimize potential side reactions and radical quenching by oxygen or protic solvents, we repeated the experiment in degassed dichloromethane instead of methanol, as well as tested other wavelengths than 365 nm, such as 308 nm, which have previously been reported for decarbonylation of cyclopropenones in triazole-fused DBCOs.¹³ Unfortunately, the results remained similar. In summary, while the pyrrolidine-fused system underwent efficient photocleavage under brief irradiation, the triazole-fused cyclopropenone required prolonged irradiation to induce decarbonylation. However, we observed radical formation and no detectable cyclooctyne, as confirmed by LC-MS and SPAAC assays, and no iEDDAC reactivity was observed. In contrast, the pyrrolidine fusion reacts cleanly, highlighting a key difference in photochemical behavior and reactivity between the two heterocyclic-fusion systems.

Discussion

A punch to the face: does scaffold fusions give dibenzocyclooctynes an edge in tetrazine ligation?

In this study, we set out to experimentally investigate computational predictions⁷ on how fusion with a five-membered nitrogen-containing heterocycle affects cyclooctyne reactivity. Incorporating a nitrogen atom offers a useful functional handle for downstream bioconjugation while maintaining the critical geometric features imparted by the cycloalkane fusion described by Svatoněk *et al.*⁷ Surprisingly, while azide reactiv-

ity is retained, the resulting pyrrolidine-fused DMBO shows no detectable reactivity toward tetrazines. This lack of tetrazine reactivity cannot be explained by common synthetic issues such as *cis/trans* isomerism or by protonation states influenced by the buffer conditions. The failure of the pyrrolidine-fused DMBO to react with tetrazines, despite DFT predictions to the contrary, highlights limitations in current computational models.

Facing the future at the edge of reactivity

While the fused nitrogen heterocycle was expected to preserve, or even enhance tetrazine reactivity, based on favorable geometric strain and electronic alignment, the complete lack of iEDDAC reactivity in the synthesized compound suggests that nitrogen incorporation introduces subtler electronic or conformational effects that are not fully captured by computational methods. Looking forward, the computational predictions by Svatoněk *et al.*⁷ indicate that fusion of a four-membered ring may provide the lowest activation barrier for tetrazine ligation among the designs tested (Fig. 1b). We propose that future studies focus on the synthesis and evaluation of this strained 4C-DMBO scaffold. Promising synthetic strategies for such four-membered ring-fused systems may include visible-light mediated [2 + 2] cycloadditions, such as those reported by Pagire *et al.*¹⁴ or cycloaddition of olefins by Liu *et al.*¹⁵

Dimethoxy substitutions versus structural alternatives

The current work has focused exclusively on the dimethoxy-DIBO scaffold previously employed by Lang and colleagues,⁶ as well as by Boons and co-workers¹² for their fluorogenic cyclooctyne. This scaffold was originally introduced by Rutjes and colleagues¹¹ through a two-step synthetic route to azadibenzocyclooctynes (ADIBO), starting from 3-ethynylanisole and 3-iodoanisole to generate two methoxy substituents on the benzene rings of the DBCO scaffold. In contrast, Popik and colleagues¹³ reported a triazole fusion on a scaffold lacking methoxy groups, derived from a Sondheimer diyne in which the 5,10-dimethoxy substituents were replaced by hydrogen or butoxy groups.¹⁶ Unexpectedly, this substitution did not yield a fluorescent compound; instead, the absorption maximum shifted from 350 nm to 310 nm, rendering the cyclopropenone cage inert to 365 nm irradiation but responsive to 308 nm light. Importantly, the resulting decarbonylation produced an intact and functional alkyne with one of the fastest reported reaction rates for cyclooctynes ($34 \text{ M}^{-1} \text{ s}^{-1}$).¹³ These findings



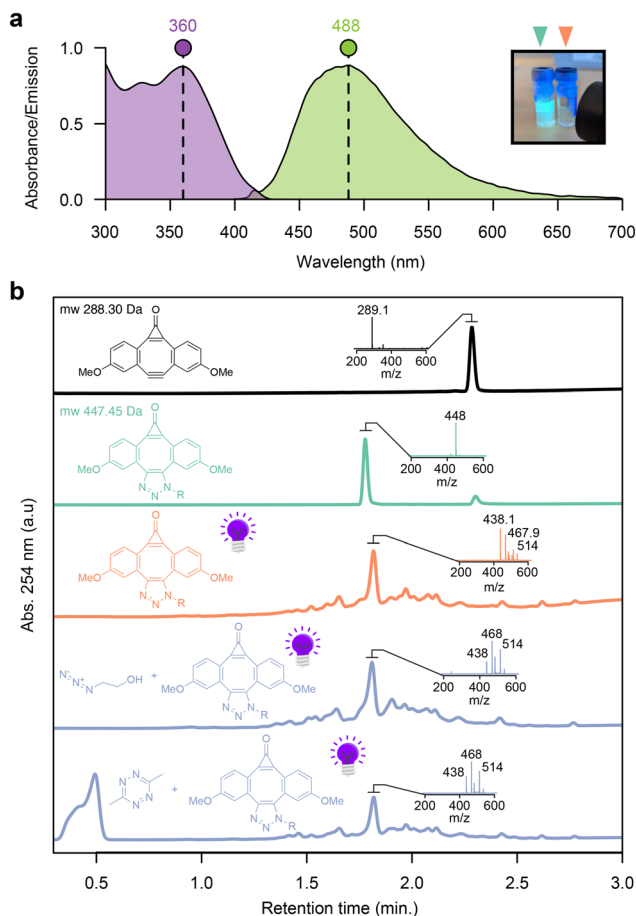


Fig. 5 Photo-triazole-DMBO produces a fluorophore, while UV decarbonylation yields radical byproducts instead of a functional alkyne. (a) Normalized absorbance and emission spectra of photo-triazole-DMBO, showing excitation maxima at 360 nm (purple) and emission maxima at 488 nm (green). Inset: photograph of methanol solutions under UV illumination, showing fluorescent photo-triazole-DMBO and non-fluorescent/bleached decarbonylated triazole-DMBO. (b) LC-MS analysis of photo-triazole-DMBO. The black trace shows the original non-fluorescent construct, FL-DIBO, reported by Boons *et al.*,¹² which converts to fluorescent photo-triazole-DMBO upon ligation with azide-PEG1-acid (turquoise trace). UV irradiation (3 mW, 100 min) produces multiple smaller LC peaks, with one dominant peak no longer corresponding to the original photo-triazole-DMBO. The associated mass spectrum reveals several new species (e.g., 438.1, 467.9, 514 *m/z*), consistent with radical byproducts from decarbonylation. Both SPAAC (with 2-azidoethanol) and iEDDAC (with 3,6-dimethyltetrazine) fail to generate the intended products (purple traces), instead showing a similar pattern of scattered peaks within the dominant LC peak (438, 468, 514 *m/z*), indicating analogous radical decomposition pathways. All reactions were performed sequentially; the azide or diene was added only after UV irradiation, and was not present during the photodecarbonylation step.

suggest that future efforts should explore whether the 5,10-dibutoxy substituents can be harnessed in iEDDAC chemistry.

Taken together, our findings highlight the utility of photo-activatable cyclooctynes as a model platform for dissecting the geometric and electronic factors governing SPAAC *versus* iEDDAC reactivity. These scaffolds offer a valuable testbed for assessing the predictive power of computational models and

for systematically exploring how ring strain and heteroatom incorporation influence cycloaddition kinetics. While recent developments in photoreactive tetrazines¹⁷ open new avenues for light-controlled iEDDAC reactions with precise temporal resolution – potentially bypassing some of the structural limitations of strained alkynes – it is important to note that tetrazine-based systems may lose their fluorogenic properties when paired with certain dye classes, such as xanthenes,¹⁸ which are critical for no-wash *in vivo* imaging. In this context, photoreactive cyclooctynes remain a compelling and complementary strategy for expanding the bioorthogonal toolbox, especially in applications requiring both fluorogenicity and spatiotemporal control. Future efforts that integrate the distinct advantages of both cyclooctyne- and tetrazine-based systems may yield versatile, high-performance reagents optimized for diverse biological settings.

Author contributions

N. A. L. conceived the synthesis route, performed the chemical synthesis, conducted experiments, analyzed data, and co-wrote the manuscript. T. J. conducted computational analysis, and contributed to manuscript writing. U. B. contributed to synthesis route suggestions, and assisted with NMR interpretation, and contributed to manuscript writing. S. C. contributed to computational analysis and provided supervision. L. R. O. provided supervision, contributed to writing, and assisted with synthesis route suggestions. D. F. supervised the project, contributed to data analysis, and wrote the manuscript.

Conflicts of interest

D. F. serves on the scientific advisory board of Navinci Diagnostics AB.

Data availability

Data for this article, including analysis and plotting scripts to reproduce figures, chemical structure files (ChemDraw), as well as raw data (LC-MS, NMR) are available in an article-associated GitHub repository at <https://github.com/furthlab/pyrrolidine-DMBO/>.

Supplementary information (SI) is available. Cartesian coordinates of *cis* isomer conformers obtained with r2SCAN-3c/CPCM(chloroform). Cartesian coordinates of *trans* isomer conformers obtained with r2SCAN-3c/CPCM(chloroform). See DOI: <https://doi.org/10.1039/d5ob01314c>.

Acknowledgements

D. F. is supported by SciLifeLab startup, SciLifeLab Technology Development Project, NARSAD Young Investigator



Grant from the Brain & Behavior Research Foundation (29810), the Chan Zuckerberg Initiative (239942), the Swedish Research Council (2022-02706), Swedish Brain Foundation (FO2022-0054), and Åke Wibergs Foundation (M22-0217). S. C. is supported by Swedish Research Council (2021-05414). The computations were enabled by resources provided by the National Academic Infrastructure for Supercomputing in Sweden (NAISS) at the Tetralith cluster (NSC in Linköping, thanks to the NAISS 2024/5-570 medium and 2025/22-1003 small compute projects) partially funded by the Swedish Research Council through grant agreement no. 2022-06725. L. R. O. is supported by Swedish Research Council (2021-03293 and 2022-04831), the Swedish Brain Foundation (FO2024-0317-HK-70) and the Swedish Cancer Society (Cancerfonden 243889 Pj).

References

- 1 N. J. Agard, J. A. Prescher and C. R. Bertozzi, *J. Am. Chem. Soc.*, 2004, **126**, 15046–15047.
- 2 X. Ning, J. Guo, M. A. Wolfert and G. Boons, *Angew. Chem., Int. Ed.*, 2008, **47**, 2253–2255.
- 3 M. L. Blackman, M. Royzen and J. M. Fox, *J. Am. Chem. Soc.*, 2008, **130**, 13518–13519.
- 4 J. Dommerholt, S. Schmidt, R. Temming, L. J. A. Hendriks, F. P. J. T. Rutjes, J. C. M. van Hest, D. J. Lefeber, P. Friedl and F. L. van Delft, *Angew. Chem., Int. Ed.*, 2010, **49**, 9422–9425.
- 5 H. E. Murrey, J. C. Judkins, C. W. am Ende, T. E. Ballard, Y. Fang, K. Riccardi, L. Di, E. R. Guilmette, J. W. Schwartz, J. M. Fox and D. S. Johnson, *J. Am. Chem. Soc.*, 2015, **137**, 11461–11475.
- 6 S. V. Mayer, A. Murnauer, M. von Wrisberg, M. Jokisch and K. Lang, *Angew. Chem., Int. Ed.*, 2019, **58**, 15876–15882.
- 7 D. Svatunek, A. Murnauer, Z. Tan, K. N. Houk and K. Lang, *Chem. Sci.*, 2024, **15**, 2229–2235.
- 8 R. Beugelmans, G. Negron and G. Roussi, *J. Chem. Soc., Chem. Commun.*, 1983, 31.
- 9 A. Poloukhine and V. V. Popik, *J. Org. Chem.*, 2003, **68**, 7833–7840.
- 10 A. A. Poloukhine, N. E. Mbua, M. A. Wolfert, G.-J. Boons and V. V. Popik, *J. Am. Chem. Soc.*, 2009, **131**, 15769–15776.
- 11 M. F. Debets, J. S. Prins, D. Merckx, S. S. van Berkel, F. L. van Delft, J. C. M. van Hest and F. P. J. T. Rutjes, *Org. Biomol. Chem.*, 2014, **12**, 5031–5037.
- 12 F. Friscourt, C. J. Fahrni and G.-J. Boons, *J. Am. Chem. Soc.*, 2012, **134**, 18809–18815.
- 13 D. A. Sutton and V. V. Popik, *J. Org. Chem.*, 2016, **81**, 8850–8857.
- 14 S. K. Pagire, A. Hossain, L. Traub, S. Kerres and O. Reiser, *Chem. Commun.*, 2017, **53**, 12072–12075.
- 15 Z. Liu, C. Zhou, T. Lei, X.-L. Nan, B. Chen, C.-H. Tung and L.-Z. Wu, *CCS Chem.*, 2020, **2**, 582–588.
- 16 D. A. Sutton, S.-H. Yu, R. Steet and V. V. Popik, *Chem. Commun.*, 2015, **52**, 553–556.
- 17 L. Liu, D. Zhang, M. Johnson and N. K. Devaraj, *Nat. Chem.*, 2022, **14**, 1078–1085.
- 18 G. Beliu, A. J. Kurz, A. C. Kuhlemann, L. Behringer-Pliess, M. Meub, N. Wolf, J. Seibel, Z.-D. Shi, M. Schnermann, J. B. Grimm, L. D. Lavis, S. Doose and M. Sauer, *Commun. Biol.*, 2019, **2**, 261.

